

Chip Flood (vs) Core Flood—Assessment of Flowback and Oil Productivity in Oil-Wet Hydraulic Fractured Rocks

Srikanth Tangirala, James J. Sheng, Jiawei Tu

Bob L. Herd Department of Petroleum Engineering, Texas Tech University, Lubbock, USA

Email: james.sheng@ttu.edu

How to cite this paper: Tangirala, S., Sheng, J.J. and Tu, J. (2019) Chip Flood (vs) Core Flood—Assessment of Flowback and Oil Productivity in Oil-Wet Hydraulic Fractured Rocks. *Open Journal of Yangtze Gas and Oil*, 4, 59-78.

<https://doi.org/10.4236/ojogas.2019.41005>

Received: October 5, 2018

Accepted: January 27, 2019

Published: January 30, 2019

Copyright © 2019 by authors and Scientific Research Publishing Inc. This work is licensed under the Creative Commons Attribution International License (CC BY 4.0).

<http://creativecommons.org/licenses/by/4.0/>



Open Access

Abstract

New developments in lab technologies help us to explore problems that were less understood in the past due to the limitations and technological constraints. One such problem of assessing the formation damage created by the invasion of fracture fluid into the matrix at lab scale is the visualization of fluid saturation distributions inside the matrix. According to the current understanding, the high capillarity contrast between the fracture and the matrix creates a non-uniform saturation distribution of invaded fluid phase during flowback, with the saturations mostly concentrated at the fracture face. With the advent of microfluidics, their application has become more feasible to visually analyze the effectiveness of surfactants to mitigate the invasion-created formation damage and understand the impact of depth of invasion on the characteristics of flowback and oil productivity. Through our previous work, we have successfully demonstrated the capability of this new visualization tool in studying the factors of the presence of surfactant in the fracture fluid and its depth of invasion, to understand the flowback efficiencies and later oil productivities in oil-wet fractured formations. Since the substrate for flooding was a proxy model of an actual rock, the chip flooding results need to be validated with conventional core flooding experiments. In contemporary times, when the new advancements in technology are driving the research progress in all industries, it is mandatory to take a well informed decision by imposing a comparative check on the results with accessible conventional means, wherever possible. The success of validation of chip flooding approach with the core flooding approach in this work instates a strong belief over the application of microfluidics to pursue more research in related fields of oil recovery.

Keywords

Chip Flooding, Core Flooding, Flowback, Fracture, Surfactant

1. Introduction

Hydraulic fracturing in horizontal wells improves the drainage area of production by creating high conductive passageway for hydrocarbon to flow from far-off regions into the wellbore. Almost 51% of US daily production is accounted to hydraulic fractured wells [1] and these production trends, in general, are predominantly dominated by fracture flow with the late-time production being supported by the matrix surrounding the fractures [2]. Due to the high injection pressures of operation, the leak-off of fracture fluids into the matrix can easily cause the constriction to the production of hydrocarbons. Moreover, these fluids could even lead to the swelling of clay particles found in the formation causing more formation damage if the flowback process is inefficient [3].

Many methods of mitigation of the leak-off or invasion-induced formation damage have been proposed by researchers. High production rates reduce the capillary entrapment of invaded fluids due to capillary desaturation and hence improve the flowback volumes. But due to the operational constraints of the surface and downhole equipment, very high production rates cannot be achieved in the field. Shut-in operation has also been explored as a possible formation damage mitigation strategy. In water-wet rocks, it is observed that the water block formed by the invaded fracture fluid predominantly exists at the matrix-fracture interface due to the capillary discontinuity between the high-permeable fracture and low-permeable matrix space surrounding it [4] [5]. Bertonecello *et al.* (2014) [6], Liang *et al.* (2015) [7], Odumabo *et al.* (2014) [8] and Yan *et al.* (2015) [9] have shown that with sufficient duration of shut-in period the water-block would imbibe away from the fracture face due to capillary redistribution resulting in improvement of relative permeability to hydrocarbon. But very long shut-in times could affect the operator adversely as the expenditures increase due to the high day-rate services offered by the service companies. Moreover, spontaneous capillary redistribution phenomenon is prominently observed in water-wet rocks and not in oil-wet rocks [10], thus raising concern over the practicality of shut-in strategies. In the case of gas reservoirs, evaporation of water block due to gas expansion has also been considered as another method of the removal of formation damage caused due to invasion [4] [5], but the time-scale of expansion-driven evaporation is significantly longer than that of displacement-driven flowback mechanism. The application of surfactants to reduce the capillary entrapment of invaded fluid has been a plausible solution suggested by Liang *et al.* (2016) [11] and Kim *et al.* (2016) [12], who demonstrated surfactant's effectiveness by conducting laboratory experiments.

Due to the dominance of high capillary pressures in fractured tight formations, the macro-scale flow dynamics are also influenced by the capillary pressure gradients acting across the fluids distributed within the formation. Longoria *et al.* (2015) [13] have shown that such a factor of capillary gradient across the invaded and uninvaded regions of low permeability matrix impacts on the reduction of formation damage as well as the flowback volumes. Similarly, the exist-

tence of high contrast in capillarity between the fracture and the matrix, aids the displacement of fracture and in-situ fluids during the production phase. Since most of the published research is concentrated on water-wet formations, the current work is catered to oil-wet fractured formations only. As discussed before, the practical strategy of mitigating the formation damage by improving the efficiency of flowback in an oil-wet formation is by using either a water-based or surfactant-based fracture fluid, rather than using shut-in procedures. Since the capillary gradient across the matrix and fracture is affected by the average invaded fluid saturation in the matrix, the invaded volume or the depth of invasion is a very crucial factor of investigation that has a direct impact on the flowback characteristics and the oil productivity from the fractured formation.

During recent times, new state-of-the-art microfluidics based tools are being used in the petroleum industry to understand the oil recovery mechanisms by visualizing the macro-scale and pore-scale fluid flow behavior in transparent microchips. Chip-scale displacement patterns, sweep efficiencies of secondary oil recovery methods using water-based fluids [14]-[19] and tertiary oil recovery methods using surfactant and polymer based fluids [20]-[29] are studied with ease using these new microfluidic based tools. He *et al.* (2017) [22] have incorporated this approach for the first time to understand the relation of flowback and invasion volumes but performed experiments with a constant rate of production, rather than using a more practical and industry-wide practice of constant pressure drop during production. Moreover, they have not considered the varying depths of invasion as another prominent factor that has a big role to play on both the lab-scale and field scale. In our previous work, Tangirala and Sheng (2018) [30] have presented microfluidic experimental results to show the impact of fracture fluid invasion on oil flow rates and flowback as a function of depth of invasion and the usage of surfactant, when invaded into an oil-wet porous space located adjacent to a fracture. It was observed that as the depth of invasion increases, the flowback efficiency decreases, irrespective of the presence of surfactant in the fracture fluid. Another important implication of that study is that for shallow invasions, the fracture fluid in the presence of surfactant does not mitigate the invasion-created formation damage better than that of the fluid without the surfactant. The applicability of these findings in the industry depends on the validity of the results in a more proven lab-scale procedure, *i.e.* using an actual core block and conducting the equivalent procedures in the domain of core flooding.

In the current work, we designed an experimental core flooding process with operating procedures similar to that used in Tangirala & Sheng (2018) [30] chip flooding method. The results are presented adjacently for both the methods to validate the microfluidic results with the core flooding results. The success of this validation methodology is an indication of the rising prominence of chip-flooding procedures which could give rise to a new technique of preliminary assessment in labs without having to work with expensive cores drilled from the subsurface.

2. Methodology

2.1. Experimental Materials

Six Berea sandstone core samples named A to F are used for core flooding whose dimensions and pore characteristics are mentioned in **Table 1**. The porosity of these samples is obtained by the weight measurement method of determination of pore volume. Permeability is also obtained by the steady-state method of flowing liquid through a 100% liquid-saturated core sample. The detailed procedures of obtaining these measurements are highlighted in the succeeding section. The core is covered with teflon tape on the curved portion to form a perfect non-invasive seal to the rubber sleeve in which it is placed. The rubber sleeve is placed inside the hassler core holder with the core tightly enclosed using the metal caps on both sides of the core holder. Besides these metal caps acting as uniform fluid distributors across the cross-sectional area of the core, they even act as a proxy for the high conductive fracture space adjoining the relatively low conductive matrix region of the porous media. Similarly, the microfluidic chip used for chip flooding is a 45 mm × 15 mm borosilicate glass chip, with a uniform channel porous network etched over it having a footprint of 20 mm × 10 mm. The chip is manufactured by Micronit Microtechnologies B.V., Netherlands. At the entry to the uniform pore network, a single wide pore channel distributes the injected fluids evenly across the whole cross sectional area of the pore network. This portion of the chip represents the fracture region where the fluid is collected first before entering into the matrix represented by the porous media channels of the chip.

The contrast in the physical dimensions of the core and the microchip is depicted in **Figure 1** as well as **Table 1** below.

Besides the core holder, the other equipment used for the core flooding process is as per the requirements such as accumulators, back pressure regulator, quizix pumps and syringe pump. But for the microfluidic experiment, the chip is housed inside a fluidic connect PRO chip holder purchased from Micronit, which is fixed over the mechanical stage of a fluorescence-imaging inverted microscope (Olympus CKX-53). The fluids are pumped using an air compressor whose pressure is controlled by a pressure based flow controller, MFCS-EZ,

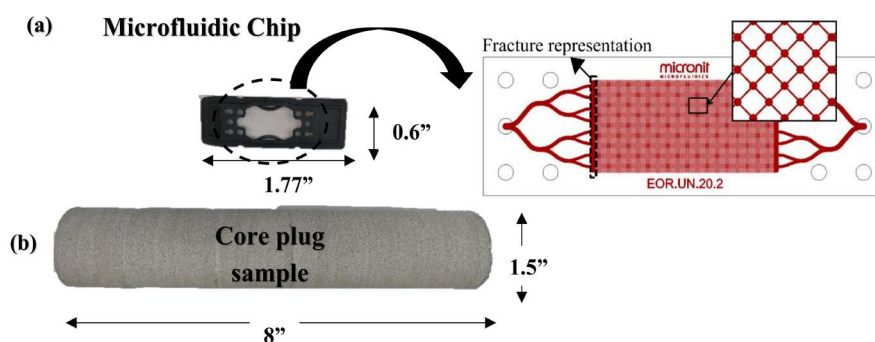


Figure 1. (a) Microfluidic chip (b) Core sample, represented along with their typical physical dimensions.

Table 1. Physical characteristics of core and chip.

Material No.	Physical Characteristics			
	Length, L /in	Diameter, D /in	K /mD	ϕ /%
Core samples				
Core-A	8	1.512	61.15	18.14
Core-B	8	1.516	53.05	17.65
Core-C	8	1.516	64.42	17.76
Core-D	8	1.514	63.88	17.76
Core-E	8	1.486	57.05	18.37
Core-F	8	1.518	59.39	17.94
Microchip				
Network of channels	0.79	0.39	2500*	60
Single channel	1.97×10^{-3} (width)	7.87×10^{-4} (depth)	-	-

*The permeability of the chip is as mentioned on the manufacturer's website:

<https://store.micronit.com/microfluidic-chips/enhanced-oil-recovery-chips/3-pack-eor-chips-uniform-net-work>.

purchased from Fluigent Inc. The flow rates in the flow lines are measured using the Flow Rate Platform (FRP) also acquired from Fluigent Inc., having a measurable range of 0 ~ 7 μ l/min. Before allowing the fluids to pass through the chip, they are filtered using a 2 μ m in-line PEEK filters provided by IDEX corporation.

The oil used in both the experiments is soltrol-130 supplied by Chevron Phillips Chemical Company having a dynamic viscosity of 2.37 cp and a specific gravity of 0.74. Deionized water (DI water) is used for conducting immiscible displacements of oil, where the IFT between soltrol oil and DI water, measured using a Du-Nuoy Ring tensiometer is 32.92 ± 0.27 mN/m. A 0.05% non-ionic surfactant supplied by ChemEOR Inc., is used for miscible displacement of soltrol oil in the chip. The observed interfacial tension (IFT) for the surfactant is 1.64 ± 0.15 mN/m, measured by the M6500 Spinning drop tensiometer purchased from Grace Instrument Company. A Fluorescein dye that is soluble only in the aqueous phase is used to distinguish between the multiple colorless fluids when they are viewed under the microscope in the microfluidic experiment. On the contrary, the saturation computation is only weight based in the core flooding experiment and hence there is no requirement of a dye to differentiate fluids for the case of core flooding experiment.

2.2. Experimental Setup & Procedure

Both of the core flooding and the chip flooding experiments are conducted at equivalent operating conditions, so that the results obtained from them are comparable. These operating conditions and the detailed procedures of operation are highlighted below.

2.2.1. Core Flooding Experimental Procedure

The schematic for the core flood experimental set up is shown in **Figure 2**.

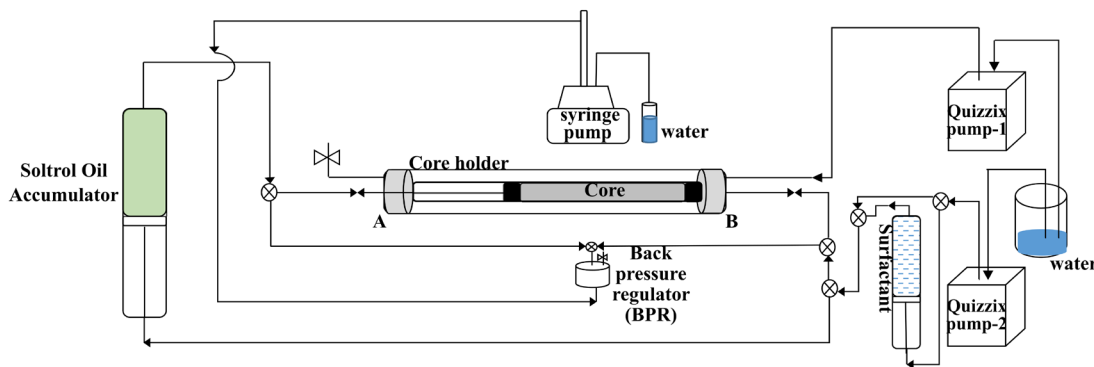


Figure 2. Schematic of core flooding set-up.

The methodology of conducting the experiment is according to the following sequence:

- **Initial saturation:** The dry core is weighed, W_d and vacuum saturated with soltrol oil (density, ρ_o) for 12 hrs in a pressurized core vessel. The weight of the oil saturated core is measured, W_o . The porosity is hence obtained according to the Equation (1). The results are tabulated in **Table 1** with the obtained porosities lying in the range of 17% ~ 19%.

$$\phi = \frac{W_o - W_d}{\rho_o} \quad (1)$$

- **Wettability assessment:** The wettability of the core is assessed by using the sessile drop method with Krüss Drop shape analyzer (DSA-25). The oil saturated core is placed in a transparent glass flask filled with oil and the wettability of the injecting fluid (either water or surfactant) is assessed by placing a droplet size portion of the fluid on the top flat surface of the core. Thereby the contact angle is obtained with oil as surrounding medium. At least 30 such instances are measured at various locations of the core to account for the heterogeneity in texture and the sample statistics thus obtained, which are enlisted in **Table 2**. Based on the results from the wettability analysis, since the mean contact angles are above 120° with a reasonable standard deviation, it can be safely inferred that the wettability of the rocks for both the water and the surfactant fluids is oil-wet.
- **Permeability assessment:** The teflon wrapped core is placed inside the core holder along with a rubber sleeve. Confining pressure of 1500 psi is applied by pumping water from quizzix pump-1. A back pressure of 900 psi is exerted on the core using a syringe pump so as to maintain a constant pressure drop of around 75 psi by pumping soltrol oil from another quizzix pump-2. The stabilized steady-state flow rate of oil is measured by collecting downstream fluid from a measuring cylinder. The effective permeability of the core is hence calculated using the Darcy's equation and the obtained results are tabulated in **Table 1**, with the range of permeability being 50 ~ 65 mD.
- **Invasion:** The forced invasion of fluid, either water or surfactant, is carried from the side B of the core holder at a constant pressure drop of 50 psi, pro-

ducing rates of around $0.1 \sim 1.5 \text{ cm}^3/\text{min}$. Since the invasion is moderately unstable displacement (viscosity ratio = 0.42), the rates are maintained, which are low to prevent any viscous fingering causing early-time breakthrough. The invading volume is varied for different cores so as to observe a trend across these varying conditions. At the end of the period of respective volume of invasion, the core is removed from the core holder and weighed again for its fluid invaded weight, W_{inv} . The invasion efficiency, $\text{inv}\%$ is hence obtained which is given by Equation (2), where V_p indicates the calculated pore volume.

$$\text{Invasion efficiency}(\text{inv}\%) = \frac{(W_{\text{inv}} - W_o)}{(\rho_w - \rho_o) \times V_p} \times 100\% \quad (2)$$

- **Flowback:** Subsequent to the invasion process, the core is placed again inside of the core holder and the oil is pumped at a constant pressure drop of 300 psi from side A of the core holder for about 10 pore volumes. The invaded fluid is ejected out as flowback and amounts pertaining to residual saturation are attained approximately after 10 PV, as observed from the measured stable oil flow rates. The pressure drop acting across the cores dictate these later oil production rates and the pressure is decided so as to obtain a comparable capillary number with that of the microfluidic experiment. At the end of the flowback phase, the core is once again removed from the core holder to measure the final weight of the core, W_{fb} .

Both the residual saturation of invaded fluid, S_{w2} and the flowback efficiency, $\text{fb}\%$ are calculated according to the Equations (3) and (4).

$$\text{Flowback Efficiency}(\text{fb}\%) = \frac{W_{\text{inv}} - W_{\text{fb}}}{W_{\text{inv}} - W_o} \times 100\% \quad (3)$$

$$S_{w2} = \frac{W_{\text{fb}} - W_o}{(\rho_w - \rho_o) \times V_p} \quad (4)$$

2.2.2. Chip Flooding Experimental Procedure

The schematic for the chip flood experimental set up is shown in **Figure 3**.

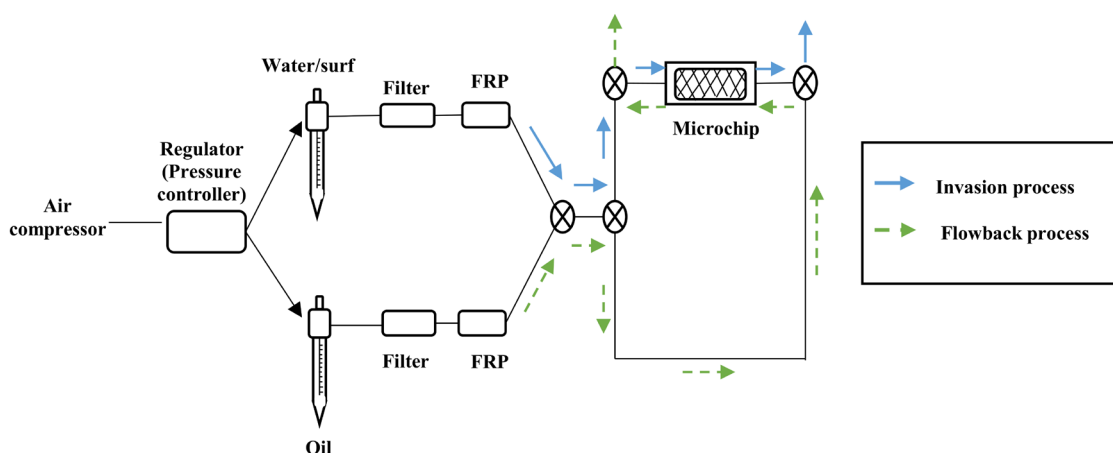


Figure 3. A schematic of chip flooding set-up.

The operational steps followed in the microfluidic experiment are similar to the core flooding case, but the same chip is used for all the varying volumes and fluids of injection. It is the advantage of working with the microchip, because the cleaning process of the chip is easier, as it requires only DI water, isopropanol and dry air as the cleaning fluid sequence, in the same order, to dispose any residual liquid particles from the porous network area of the chip.

The following steps are followed in the chip flooding experimentation:

- **Wettability assessment:** A clean and dry chip is saturated with either DI water or surfactant completely, subsequent to which soltrol oil is injected at 80 mbar pressure till residual ganglia of the water or surfactant are formed all throughout the chip. Due to the presence of fluorescein dye, the aqueous phase is differentiated against the non-aqueous phase when viewed under a fluorescence microscope with UV illumination. To understand the uniformity of the wetting characteristic of the chip, 40 measurements of contact angles are taken at regular intervals across the whole area of the chip and sample statistics are tabulated in **Table 2**. The wettability of the chip is clearly inferred to be oil-wet when water is the non-wetting phase, but with surfactant the mean contact angle is slightly lowered below 120° with relatively higher standard deviation. It indicates that barring a few areas which are rendered mildly neutral wetting due to the surfactant, the in-general wetting characteristic of the chip is oil-wet. A pictorial instance of contact angle measurement along the surface of the chip and the fluid ganglia is shown in **Figure 4(a)**, showing the oil-wetting nature of the chip. For comparison, a representative instance of contact angle measurement between the liquid droplet and the core block is also shown in **Figure 4(b)**.
- **Invasion:** The chip is cleaned again and dried with air for a long time. Soltrol oil is injected to completely saturate the chip, so as to attain the same initial condition as the core in the core flooding experiment. A required volume of invading fluid, either water or surfactant, is injected at 80 mbar pressure into the chip along the flow path indicated by the blue solid arrows in **Figure 3**. Subsequently, the valves at the inlet and the outlet of the chip are closed to

Table 2. Contact angle measures for wettability assessment.

Material No.	Water wettability		Surfactant wettability	
	Mean contact angle/(°)	Std Dev/(°)	Mean contact angle/(°)	Std Dev/(°)
Core-A	135.47	14.69	-	-
Core-B	131.36	10.33	-	-
Core-C	126.6	16.42	-	-
Core-D	-	-	140.42	14.2
Core-E	-	-	139.73	10.56
Core-F	-	-	127.83	11.77
Microchip	125.35	15.73	116.08	25.89

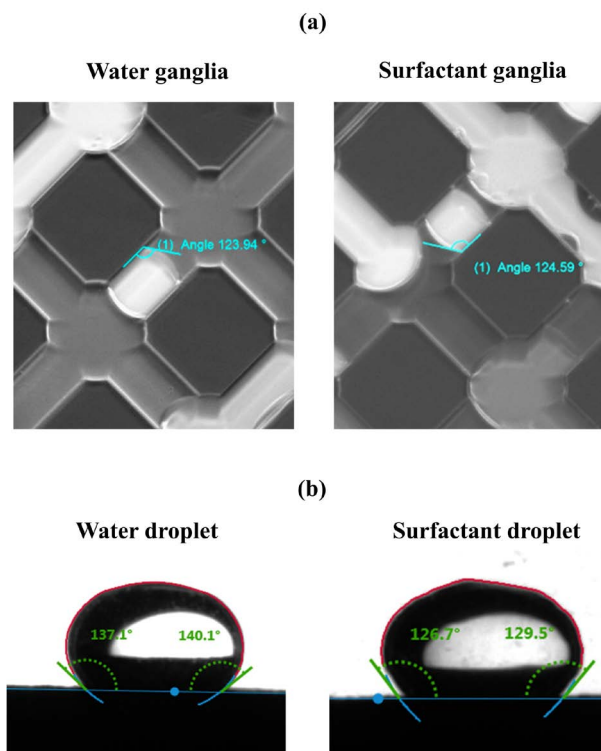


Figure 4. A representative instance of (a) Contact angle of water (left) and surfactant (right) against the oil media and the chip surface (b) Contact angle between the water droplet (left) and surfactant droplet (right) against the core surface.

acquire the image of the whole chip from the microscope. A 2x objective lens is used to capture the individual images of the adjacent portions of the chip which are then manually stitched together using Olympus STREAM software. The image thus attained is processed further to obtain the saturation of the invaded phase, S_{w1} .

- **Flowback:** Soltrol oil is reinjected into the chip, but from the opposite direction indicated by the green dashed arrows in **Figure 3** at the same pressure of 80 mbar. After approximately 10 PV (pore volumes) of injection, the invaded phase saturation attains residual level, upon visual inspection, and immediately the final stabilized oil rate, Q_0 is measured using the FRP. The later oil production rates indicate the relative amount of reduction of formation damage caused due to the invasion phenomenon. The justification for applying such low injection pressures could be obtained after evaluating the capillary numbers from these production rates that lie in the order of 10^{-5} . These capillary numbers are typical for the formations where capillary forces begin to show their dominance [23]. The valves at the both ends of the chip are closed once again and the image of the whole chip is acquired to calculate the final saturation of the invaded fluid, S_{w2} . Based on the measured saturations, the invasion efficiency and the flowback efficiencies can be directly calculated from Equations (5) and (6).

$$\text{Invasion efficiency (inv\%)} = S_{w1} \times 100\% \quad (5)$$

$$\text{Flowback efficiency (flb\%)} = \frac{S_{w1} - S_{w2}}{S_{w1}} \times 100\% \quad (6)$$

- **Image processing:** The stitched image of the entire chip is cropped at the boundary of the porous media and is converted to a binary image format using Image J software. The saturations of the fluids inside the chip are thus computed by analyzing the histogram of the black and the white colored pixels of the binary image.

3. Results and Discussion

The experimental results for both the chip-flooding and core-flooding methods are tabulated in **Table 3** and **Table 4** respectively. The trends obtained from both of the methods are evaluated simultaneously to qualitatively validate the observations arising from the similar experimental procedures, as mentioned in the previous section. With reference to the previous results obtained for chip-flooding from Tangirala & Sheng (2018) [30], the addition of surfactant to the fracture fluid shows a contrasting behavior to the fluid without the surfactant, at varying depths of invasion. These factors are hence dealt individually in the following section to better understand the effects of their variabilities.

Table 3. Summary of microfluidic experimental results.

Invasion fluid	Chip-flooding Experimental data				
	Invasion/%	$S_{w2}/1$	Flowback/%	$Q_o/ (\mu\text{-min}^{-1})$	$N_{ca} (\times 10^{-5})$
Water	12.14	0.004	96.97	2.949	2.855
	16.65	0.031	81.43	3.255	3.151
	20.45	0.007	97.71	4.366	4.226
	39.65	0.141	64.40	1.801	1.743
	45.11	0.353	21.66	0.000	0.000
Surfactant	11.61	0.023	80.00	2.468	48.97
	17.21	0.040	76.84	2.800	55.56
	42.46	0.158	62.72	2.186	43.37
	48.61	0.196	59.68	1.260	25.00

Table 4. Summary of core flooding experimental results.

Invasion fluid	Core. No	Core-flooding Experimental data				
		Invasion/%	$S_{w2}/1$	Flowback/%	$Q_o/ (\text{cc}\cdot\text{min}^{-1})$	$N_{ca} (\times 10^{-5})$
Water	Core A	25.82	0.129	50	17.93	10.221
	Core B	32.47	0.193	40.63	12.83	7.472
	Core C	46.39	0.303	34.78	11.25	6.744
Surfactant	Core D	26.30	0.152	42.31	15.70	188.15
	Core E	37.55	0.233	37.84	12.96	161.15
	Core F	43.83	0.27	38.64	12.44	148.17

3.1. Effect of Depth of Invasion in the Absence of Surfactant

The processed microchip images, depicted in **Figure 5**, after both the invasion and the flowback phases with water as the invading fluid, can be visually analyzed for saturation information *i.e.* S_{w1} and S_{w2} . But for core flooding experiments, such information is derived from the weight measurements due to the lack of availability of CT scanner with better resolving capabilities. As discussed in the previous section, the invasion and flowback efficiency for chip flooding experiment are derived from Equations (2) and (3), whereas for the core flooding experiment, they are derived from Equations (5) and (6).

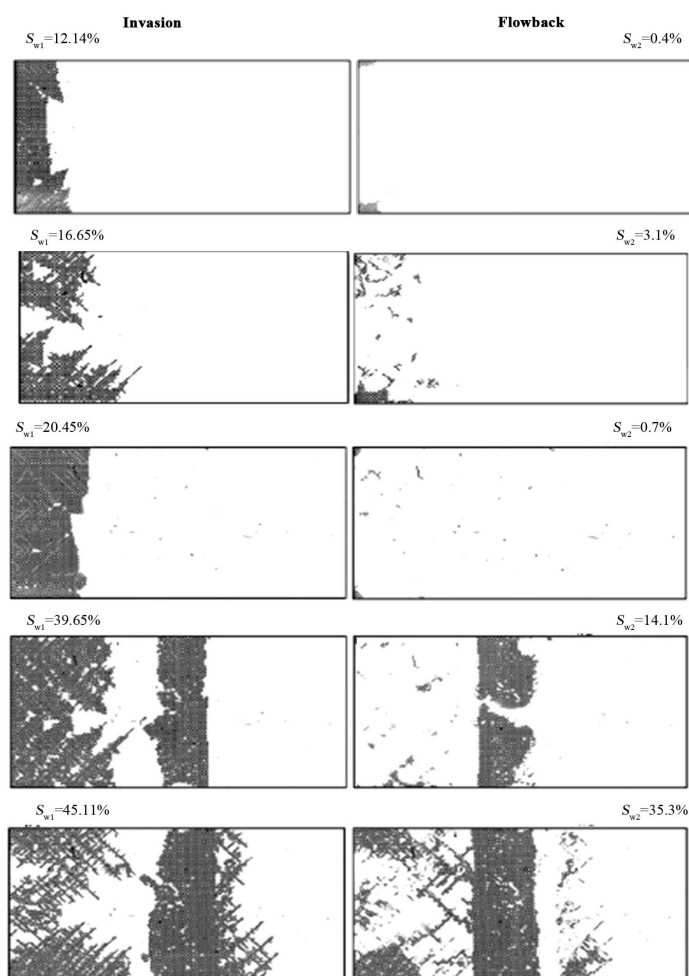


Figure 5. Water as invaded fluid (represented by black color) for an oil-wet chip, showcasing the stitched microchip images after invasion (left column) and after flowback (right column) for different invasion efficiencies.

The relationships of the invasion efficiency with both the residual saturation of the invaded fluid (S_{w2}) and the final stabilized oil production rates after flowback (Q_o), for the processes of chip flooding and core flooding are shown in **Figure 6** and **Figure 7** respectively.

For the purpose of simple qualitative comparison, linear trendlines are plotted over the data points due to the unknown nature of the degree of relationship of

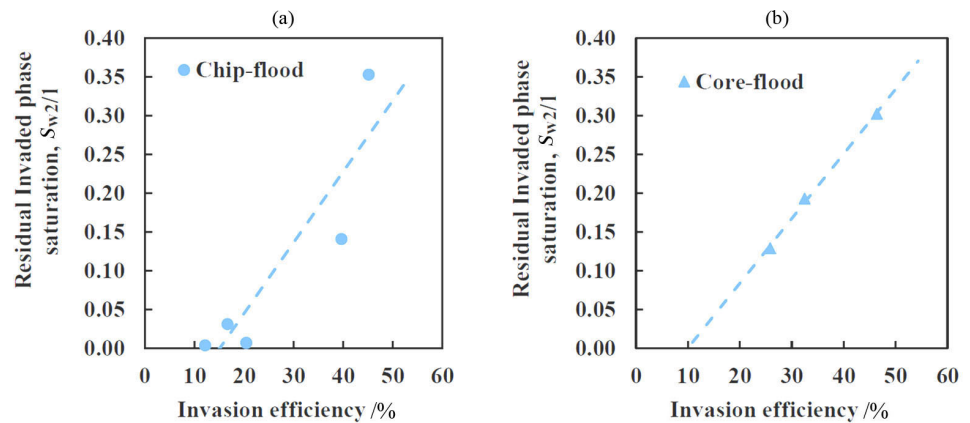


Figure 6. Relationship between S_{w2} and invasion efficiency for (a) Chip flood (b) Core flood, in the absence of surfactant.

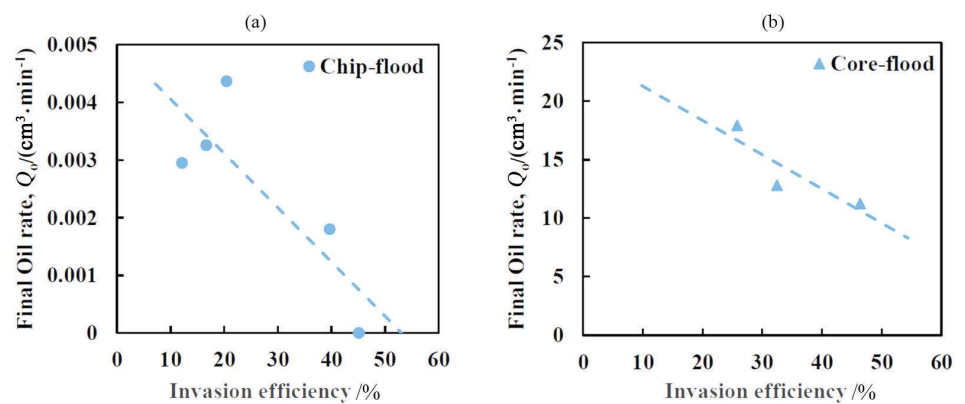


Figure 7. Relationship between final stabilised oil rate after flowback and invasion efficiency for (a) Chip flood (b) Core flood, in the absence of surfactant.

the mentioned parameters beforehand. Even though the invasion efficiency is a volumetric quantity, it can be fairly translated to the depth of invasion due to the low injection pressure application in both the methods preventing viscous fingering. Such an approximation could even be supported by the uniform sweeping pattern of invasion across the cross sectional area of the porous network of the chip visualized in [Figure 5](#).

From [Figure 6](#), it can be seen that both the processes of chip flooding and core flooding exhibit similar direct proportionality of relation of S_{w2} with invasion efficiency. It can be attributed to the increase in the capillary trapping of the invading fluid within the pores as a larger amount of fracture fluid is injected. Such increase in the residual saturations of the fracture fluid results in a reduction in the relative permeability of oil which is reflected as formation damage and hence the later oil production rates could also be severely affected. This trend is clearly depicted in [Figure 7](#) for both the processes of chip flooding and core flooding where a decreasing trend for Q_o is observed as invasion efficiency is increased. Henceforth, these results could be interpreted to state that as the depth of invasion of the fracture fluid into the oil-wet matrix increases, the tendency for the reduction of formation damage due to flowback decreases.

To better understand the characteristic of the flowback process, the invasion efficiency is cross plotted against flowback efficiency, as shown in **Figure 8**.

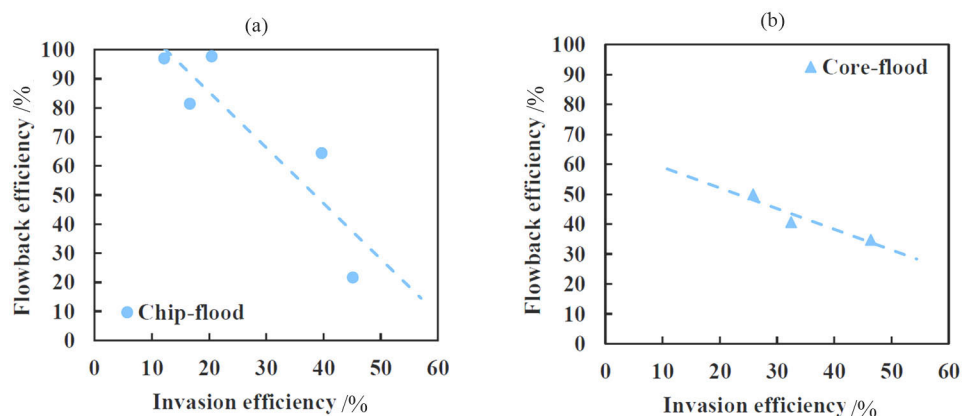


Figure 8. Relationship between flowback efficiency and invasion efficiency for (a) Chip flood (b) Core flood, in the absence of surfactant.

Both the experimental methods of chip flood and core flood showcase the same inverse proportionality of the relation between invasion efficiency and flowback efficiency. It indicates that for the case of shallow depth of invasion, the flowback efficiency is more relative to the deeper depth of invasion. Such a non-uniform nature of distribution of the residual saturations of the invaded phase across the oil-wet surface can be attributed to the existence of the capillary pressure discontinuity between the high conductive fracture and the low conductive matrix space. The saturation of the connected water phase is reduced to the lowest near the fracture face due to the additional capillary gradient driving force acting across the matrix-fracture interface, thus resulting in high flowback efficiency at shallow invasions. Conversely, at deeper invasions, the influence of this additional driving force is decreased due to the distance away from the matrix-fracture interface, causing a decrement in the flowback efficiency.

Since the qualitative trends observed in both the core flooding and the chip flooding processes are the same as seen in the **Figures 6-8**, the physical phenomena expected to be seen in the core flooding are well represented in the process of chip flooding too. It provides a lucrative opportunity for the petroleum industry to substitute the time-consuming and relatively expensive core flooding experiments with the inexpensive chip flooding application to study the outcome of the interactions of fracture fluids with the in-situ fluids at various initial and operating conditions.

3.2. Effect of Depth of Invasion in the Presence of Surfactant

The processed microchip images after both the invasion and the flowback phases with surfactant as the invading fluid can be visualized in **Figure 9**.

A non-ionic surfactant is added to the fracture fluid, due to its non-aggressive nature in changing the wettability of the chip and the core, as evidenced from **Table 2**. Most of the commercially available non-ionic surfactants reduce the

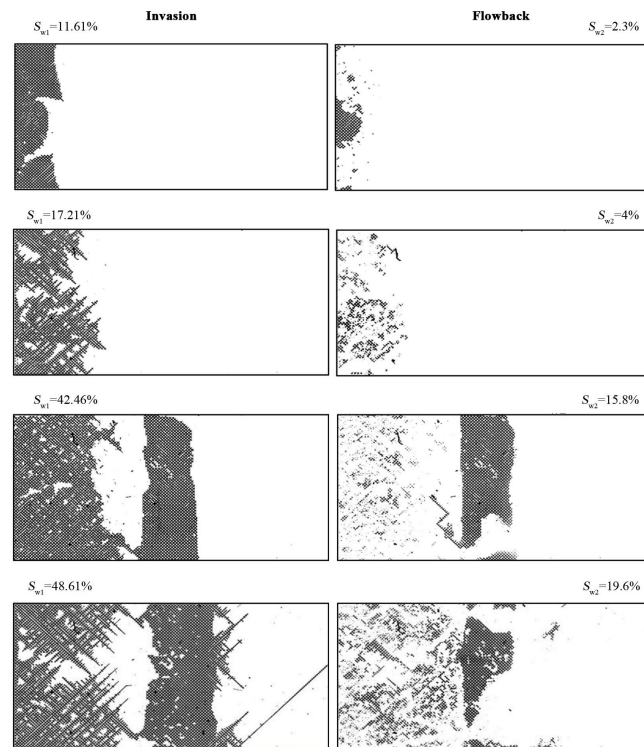


Figure 9. Surfactant as invading fluid (represented by black color) for an oil-wet chip, showcasing the stitched microchip images after invasion (left column) and after flowback (right column) for different invasion efficiencies.

IFT between the fluids moderately, whereas ultra-low IFT is achieved only under certain specific concentrations and salinities. The application of such a moderately IFT-reducing surfactant in our case reduces the interfacial tension by one order of magnitude and hence increases the capillary number similarly. The presence of such a surfactant in the fracture fluid is studied in this section where the dependency of depth of invasion into the matrix upon the flowback efficiency and oil productivity is being established. The following **Figures 10-12**, represent such relations of both the processes of chip flood and core flood.

The relationships of the depth of invasion of the fluid in the presence of

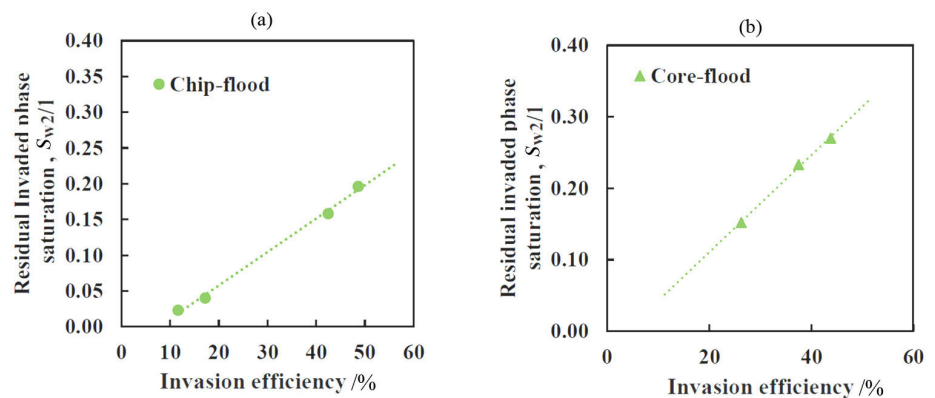


Figure 10. Relation between S_{w2} and invasion efficiency for (a) Chip flood and (b) Core flood, in the presence of surfactant.

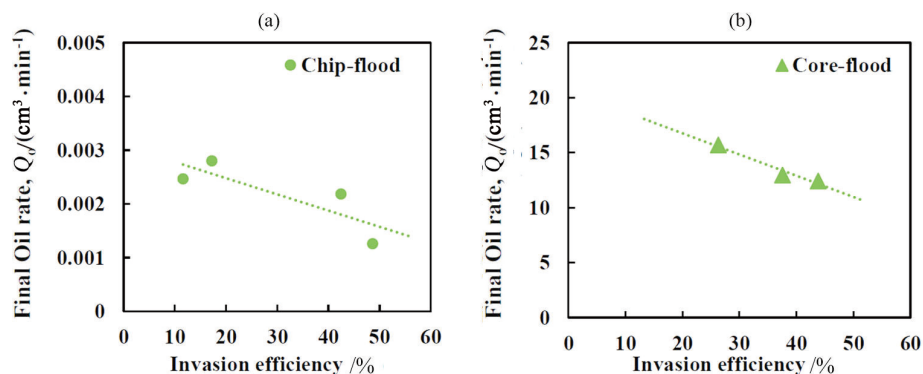


Figure 11. Relation between final stabilised oil rate and invasion efficiency for (a) Chip flood and (b) Core flood, in the presence of surfactant.

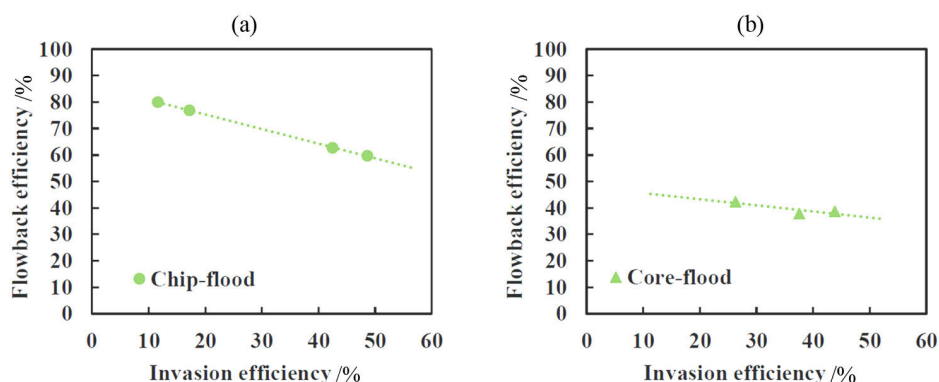


Figure 12. Relation between flowback efficiency and invasion efficiency for (a) Chip flood and (b) Core flood, in the presence of surfactant.

surfactant with S_{w2} , Q_o and flowback efficiency are all the same as observed for the case of the fluid in the absence of surfactant. Moreover, both the core flood and chip flood once again follow the same trend behaviors in each case. These observations once again bolster our inferences made about substituting the cumbersome core flooding methods with easily manageable chip flooding application.

3.3. Effect of Surfactant Addition to Fracture Fluid at Fixed Invasion Depth

The previous analyses highlight the influence of the invasion efficiencies or invasion depths of the fracture fluid, considering the absence and the presence of the surfactant independently. They establish the overall behavior of the parameters of later oil production rates, residual saturation of invaded fluid and the flowback efficiency for an oil-wetting surface. The capillary gradient across the matrix and the fracture is considered accountable for the decreasing flowback efficiency trend with respect to the invasion depth. Since the strength of the capillary gradient depends on the capillary pressure in the matrix, the presence of the surfactant could depreciate such an effect where it is prominent. Therefore, the performance of the two types of fracture fluids *i.e.* water and the surfactant are compared together at fixed invasion efficiencies to prove their contrasting beha-

avior. Such an analysis is once again studied for both the core flooding as well as chip flooding experiments and it is based on the similarity of results obtained in preceding sections. It is expected that both these methods yield similar qualitative results.

For the ease of comparative analysis, new parameters of X , Y and Z are defined which give the difference in the values of S_{w2} , flowback% and Q_o , respectively, between the water and surfactant, normalized by their respective maximum value of differences. These parameters of X , Y , and Z are defined by Equations (7)-(9), which are obtained at fixed invasion efficiencies with the aid of linearly regressed models of S_{w2} , Q_o and flowback% parameters obtained from **Figures 6-8** and **Figures 10-12**.

$$X = \frac{(S_{w2})_{\text{water}} - (S_{w2})_{\text{surf}}}{|(S_{w2})_{\text{water}} - (S_{w2})_{\text{surf}}|_{\text{max}}} \quad (7)$$

$$Y = \frac{(flb)_{\text{surf}} - (flb)_{\text{water}}}{|(flb)_{\text{surf}} - (flb)_{\text{water}}|_{\text{max}}} \quad (8)$$

$$Z = \frac{(Q_o)_{\text{surf}} - (Q_o)_{\text{water}}}{|(Q_o)_{\text{surf}} - (Q_o)_{\text{water}}|_{\text{max}}} \quad (9)$$

The values of X , Y , and Z for the selected fixed invasion efficiencies are shown in **Figure 13(a)** and **Figure 13(b)** for chip flooding and core flooding experiments, respectively.

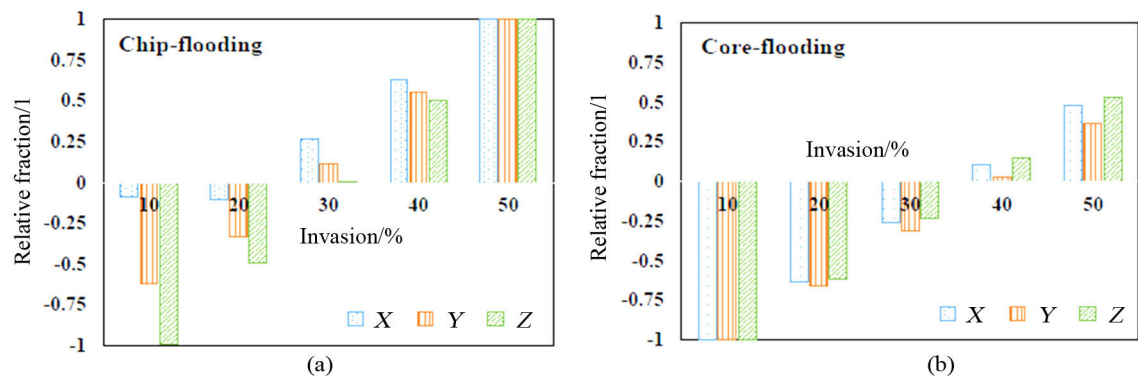


Figure 13. Relative performance of fracture fluid with surfactant against the one without surfactant for both (a) Chip flood and (b) Core flood experiments.

With respect to both the methods of experimentation, it can be observed that there is a certain critical amount of invasion below which the performance of surfactant fluid in reducing the formation damage is lower than that of the fluid without the surfactant. For chip flooding experiment, the critical invasion efficiency lies between 20% and 30% and for the core flooding experiment, it lies between 30% and 40%. Even though the determination of factors that influence this critical point of invasion is not the current scope of study, qualitatively both the methods of experimentation evidently show the existence of such a critical point. The influence of the previously discussed matrix-fracture capillary gra-

dient could be seen to be prominent for the invasions below this critical point. Hence, at shallow invasions, as the capillary gradient is reduced by the presence of the surfactant in the fracture fluid, the quantities of X , Y and Z representing the relative superiority in the performance of the surfactant are negative. But at deep invasion, as the strength of the capillary gradient across the matrix and the fracture is lesser pronounced, the X , Y and Z are all observed to be positive, indicating that the surfactant is more beneficial to be included in the fracture fluid than be excluded. It could be attributed to the better mobilization of residual saturations by capillary desaturation effect of the surfactant in the fracture fluid, as it increases the capillary number by approximately one order of magnitude (Table 3 and Table 4) and hence reduces the residual saturation of invaded fluid trapped in the pore space better than the fluid without the surfactants.

The resemblance of the trend in results for both the chip flooding and core flooding experiments indicates that customized microfluidic experiments could in fact be used as a precursor of core flooding experiments to understand the qualitative behavior of interaction of fracture fluids with both the in-situ fluids as well as the complex porous network of subsurface in terms of sweep efficiency, oil recovery, flowback potential etc. The recent advances in fabrication of chips [29] also expose a whole new domain to improve the scope of research so as to understand the flow dynamics in unconventional formations such as shales.

4. Conclusions

The microfluidic results published in the previous work [30], indicate that irrespective of the presence of moderate IFT-reducing surfactant in the fracture fluid, an increment in the depth of invasion into the matrix has yielded a decrement in the later oil production rates and flowback efficiencies. Thus, the reduction of invasion-created formation damage during flowback is more difficult when the invasion is deeper. Moreover, the microfluidic results also indicate that moderate IFT-reducing surfactants are beneficial to reduce the formation damage only when the invasion is deep; and their formation damage is even higher than water when the invasion is shallow. These results were only obtained previously for the case of a chip which acted as a proxy for the physical subsurface rock. The present study thus validates these microfluidic results by following similar procedures of invasion and flowback under equivalent operating conditions in a core flooding set-up, with the chip being replaced by an actual core plug. The results obtained for the core flooding experiments qualitatively resemble the results obtained for the chip flood experiments, both in terms of the effect invasion depth as well as the effect of a moderate IFT-reducing surfactant in the fracture fluid.

Hence, it could be safely said that the assessment of flowback and oil productivities for an oil-wet hydraulic fractured formation could be performed through chip flooding before core flooding and the results could be relied upon with equal confidence.

Conflicts of Interest

The authors declare no conflicts of interest regarding the publication of this paper.

References

- [1] Cook, T. and Perrin, J. (2016) Hydraulic Fracturing Accounts for about Half of Current U.S. Crude Oil Production. <https://www.eia.gov/todayinenergy/detail.php?id=25372>
- [2] Guo, B. and Schechter, D.S. (1997) A Simple and Rigorous Mathematical Model for Estimating Inflow Performance of Wells Intersecting Long Fractures. *Proceedings of the SPE Asia Pacific Oil and Gas Conference and Exhibition*, Kuala Lumpur, Malaysia, 14-16 April 1997, 645-659. <https://doi.org/10.2118/38104-MS>
- [3] Gupta, N., Rai, C.S. and Sondergeld, C.H. (2013) Petrophysical Characterization of the Woodford Shale. *Petrophysics*, **54**, 368-382.
- [4] Kamath, J. and Laroche, C. (2003) Laboratory-Based Evaluation of Gas Well Deliverability Loss Caused by Water Blocking. *SPE Journal*, **8**, 71-80. <https://doi.org/10.2118/83659-PA>
- [5] Mahadevan, J. and Sharma, M. (2005) Factors Affecting Cleanup of Water Blocks: A Laboratory Investigation. *SPE Journal*, **10**, 238-246. <https://doi.org/10.2118/84216-PA>
- [6] Bertoncetto, A., Wallace, J., Blyton, C., Honarpour, M. and Kabir, C.S. (2014) Imbibition and Water Blockage in Unconventional Reservoirs: Well Management Implications during Flowback and Early Production. *SPE Reservoir Evaluation & Engineering*, **17**, 497-506. <https://doi.org/10.2118/167698-PA>
- [7] Liang, T., Longoria, R.A., Lu, J., Nguyen, Q.P. and Dicarolo, D.A. (2015) Enhancing Hydrocarbon Permeability after Hydraulic Fracturing: Laboratory Evaluations of Shut-Ins and Surfactant Additives. *Proceedings of the SPE Annual Technical Conference and Exhibition*, Houston, 28-30 September 2015, SPE-175101. <https://doi.org/10.2118/175101-MS>
- [8] Odumabo, S.M., Karpyn, Z.T. and Ayala, L.H. (2014) Investigation of Gas Flow Hindrance Due to Fracturing Fluid Leakoff in Low Permeability Sandstones. *Journal of Natural Gas Science and Engineering*, **17**, 1-12. <https://doi.org/10.1016/j.jngse.2013.12.002>
- [9] Yan, Q., Lemanski, C., Karpyn, Z.T. and Ayala, L.F. (2015) Experimental Investigation of Shale Gas Production Impairment Due to Fracturing Fluid Migration during Shut-In Time. *Journal of Natural Gas Science and Engineering*, **24**, 99-105. <https://doi.org/10.1016/j.jngse.2015.03.017>
- [10] Liang, T., Zhou, F., Lu, J., DiCarlo, D. and Nguyen, Q. (2017) Evaluation of Wettability Alteration and IFT Reduction on Mitigating Water Blocking for Low-Permeability Oil-Wet Rocks after Hydraulic Fracturing. *Fuel*, **209**, 650-660. <https://doi.org/10.1016/j.fuel.2017.08.029>
- [11] Liang, T., Achour, S.H., Longoria, R.A., Dicarolo, D.A. and Nguyen, Q.P. (2016) Identifying and Evaluating Surfactant Additives to Reduce Water Blocks after Hydraulic Fracturing for Low-Permeability Reservoirs. *Proceedings of the SPE Improved Oil Recovery Conference*, Tulsa, 11-13 April 2016, SPE 179601.
- [12] Kim, J., Goma, A.M., Nelson, S.G. and Hudson, H.G. (2016) Engineering Hydraulic Fracturing Chemical Treatment to Minimize Water Blocks: A Simulated Reservoir-on-Chip Approach. *Proceedings of the SPE International Conference & Exhi-*

- bition on Formation Damage Control*, Lafayette, Louisiana, 24-26 February 2016, SPE 178959.
- [13] Longoria, R.A., Liang, T., Nguyen, Q.P. and Dicarolo, D.A. (2015) When Less Flowback Is More: A Mechanism of Permeability Damage and Its Implications on the Application of EOR Techniques, *Proceedings of the Unconventional Resources Technology Conference*, San Antonio, 20-22 July 2015, SPE-178583.
- [14] Cottin, C., Bodiguel, H. and Colin, A. (2010) Drainage in Two Dimensional Porous Media: From Capillary Fingering to Viscous Flow. *Physical Review E*, **82**, Article ID: 046315. <https://doi.org/10.1103/PhysRevE.82.046315>
- [15] Lenormand, R., Touboul, E. and Zarcone, C. (1988) Numerical Models and Experiments on Immiscible Displacement in Porous Media. *Journal of Fluid Mechanics*, **189**, 165-187. <https://doi.org/10.1017/S0022112088000953>
- [16] Razmavar, I., Alami, F.M., Rasaei, M.R. and Nadafpour, M. (2017) Microscopic Fractal-Dimension Study of Rate and Viscosity Changes on Displacement Pattern by Use of 2D Glass Micromodel. *SPE Reservoir Evaluation & Engineering*, **20**, 8-18. <https://doi.org/10.2118/181752-PA>
- [17] Tsakiroglou, C.D., Avraam, D.G. and Payatakes, A.C. (2007) Transient and Steady State Relative Permeabilities from Two Phase Flow Experiments in Planar Pore Networks. *Advances in Water Resources*, **30**, 1981-1992. <https://doi.org/10.1016/j.advwatres.2007.04.002>
- [18] Unsal, E., Hammond, P. and Schneider, M. (2011) Effects of Surfactant on Wettability and Oil Recovery in a Pore Network Model. *Proceedings of the 16th European Symposium on Improved Oil Recovery*, European Association of Geoscientists and Engineers, Cambridge, 12-14 April 2011, 61-74.
- [19] Zhang, C., Oostrom, M. and Wietsma, T.W. (2011) Influence of Viscous and Capillary Forces on Immiscible Fluid Displacement: Pore Scale Experimental Study in a Water Wet Micromodel Demonstrating Viscous and Capillary Fingering. *Energy & Fuels*, **25**, 3493-3505. <https://doi.org/10.1021/ef101732k>
- [20] Clarke, A., Howe, A.M., Mitchell, J. and Staniland, J. (2015) Mechanism of Anomalous Increased Oil Displacement with Aqueous Viscoelastic Polymer Solutions. *Soft Matter*, **11**, 3536-3541. <https://doi.org/10.1039/C5SM00064E>
- [21] Hammond, P.S. and Unsal, E. (2012) A Dynamic Pore Network Model for Oil Displacement by Wettability Altering Surfactant Solution. *Transport in Porous Media*, **92**, 789-817. <https://doi.org/10.1007/s11242-011-9933-4>
- [22] He, K., Xu, L., Kenzekanov, S., Yin, X. and Neeves, K.B. (2017) Rock-on-a-Chip Approach to Study Fluid Invasion and Flowback in Liquid Rich Shale Formations. *Proceedings of the SPE Oklahoma City Oil and Gas Symposium*, Oklahoma City, 27-31 March 2017, SPE 185088.
- [23] Xu, W., Ok, J.T., Xiao, F., Neeves, K.B. and Yin, X. (2014) Effect of Pore Geometry and Interfacial Tension on Water-Oil Displacement Efficiency in Oil Wet Microfluidic Porous Media Analogs. *Physics of Fluids*, **26**, Article ID: 093102. <https://doi.org/10.1063/1.4894071>
- [24] Howe, A.M., Clarke, A., Mitchell, J., Staniland, J. and Hawkes, L.A. (2015) Visualizing Surfactant EOR in Core Plugs and Micromodels. *Proceedings of the SPE Enhanced Oil Recovery Conference*, Kuala Lumpur Malaysia, 11-13 August 2015, SPE 174643.
- [25] Ibrahim, A.S. (2009) Investigation of the Mobilization of Residual Oil Using Micromodels. *Proceedings of the SPE Annual Technical Conference and Exhibition*, New Orleans, 4-7 October 2009, SPE 129515.
- [26] Nilsson, M.A., Kulkarni, R., Gerberich, L., Hammond, R., Singh, R., Baumhoff, E.

- and Rothstein, J.P. (2013) Effect of Fluid Rheology on Enhanced Oil Recovery in a Microfluidic Sandstone Device. *Journal of Non Newtonian Fluid Mechanics*, **202**, 112-119. <https://doi.org/10.1016/j.jnnfm.2013.09.011>
- [27] Rock, A., Hincapie, R.E., Wegner, J. and Ganzer, L. (2017) Advanced Flow Behavior Characterization of Enhanced Oil Recovery Polymers Using Glass-Silicon-Glass Micromodels That Resemble Porous Media. *Proceedings of the SPE Europec 79th EAGE Conference and Exhibition*, Paris, 12-15 June 2017, SPE-185814.
- [28] Wegner, J. and Ganzer, L. (2017) Rock-on-a Chip Devices for High P, T Conditions and Wettability Control for the Screening of EOR Chemicals. *Proceedings of the SPE Europec featured at 79th EAGE Conference and Exhibition*, Paris, France, 12-15 June 2017, SPE-185820.
- [29] Xu, K., Liang, T., Zhu, P., Qi, P., Lu, J., Huh, C. and Balhoff, M. (2017) A 2.5-D Glass Micromodel for Investigation of Multi-Phase Flow in Porous Media. *Lab on a Chip*, **17**, 640-646. <https://doi.org/10.1039/C6LC01476C>
- [30] Tangirala, S. and Sheng, J. (2018) Effects of Invasion of Water with and without Surfactant on the Oil Production and Flowback through an Oil Wet Matrix—A Microfluidic Chip Based Study. *Open Journal of Yangtze Gas and Oil*, **3**, 278-292. <https://doi.org/10.4236/ojogas.2018.34024>